HHS Public Access

Author manuscript

Mucosal Immunol. Author manuscript; available in PMC 2020 January 15.

Published in final edited form as:

Mucosal Immunol. 2019 September ; 12(5): 1174–1186. doi:10.1038/s41385-019-0189-6.

Anti-IL-13Rα2 therapy promotes recovery in a murine model of inflammatory bowel disease

E. P. Karmele[1,2], **T. S. Pasricha**[1], **T. R. Ramalingam**[1], **R. W. Thompson**[1], **R. L. Gieseck III**[1,3], **K. J. Knilans**[1], **M. Hegen**[3], **M. Farmer**[4], **F. Jin**[4], **A. Kleinman**[5], **D. A. Hinds**[5], **The 23andMe Research Team**[5], **T. Almeida Pereira**[1], **R. de Queiroz Prado**[1,3], **N. Bing**[6], **L. Tchistiakova**[4], **M. T. Kasaian**[3], **T. A. Wynn**[1,3], **K. M. Vannella**[1]

[1]Immunopathogenesis Section, Laboratory of Parasitic Diseases, National Institute of Allergy and Infectious Diseases, National Institutes of Health, Bethesda, MD, USA

[2]Institute for Biomedical Sciences, The George Washington University, Washington, DC, USA

[3]Inflammation and Immunology Research Unit, Pfizer Inc., Cambridge, MA, USA

[4]Biomedicine Design, Pfizer Inc., Cambridge, MA, USA

[5]23andMe, Mountain View, CA, USA

[6]Human Genetics, Pfizer Inc., Cambridge, MA, USA

Abstract

There continues to be a major need for more effective inflammatory bowel disease (IBD) therapies. IL-13Rα2 is a decoy receptor that binds the cytokine IL-13 with high affinity and diminishes its STAT6-mediated effector functions. Previously, we found that IL-13Rα2 was necessary for IBD in mice deficient in the anti-inflammatory cytokine IL-10. Here, we tested for the first time a therapeutic antibody specifically targeting IL-13Rα2. We also used the antibody and *Il13ra2*$^{-/-}$ mice to dissect the role of IL-13Rα2 in IBD pathogenesis and recovery. *Il13ra2*$^{-/-}$ mice were modestly protected from induction of dextran sodium sulfate (DSS)-induced colitis. Following a seven-day recovery period, *Il13ra2*$^{-/-}$ mice or wild-type mice administered the IL-13Rα2-neutralizing antibody had significantly improved colon health compared to control mice. Neutralizing IL-13Rα2 to increase IL-13 bioavailability promoted resolution of IBD even if neutralization occurred only during recovery. To link our observations in mice to a large human cohort, we conducted a phenome-wide association study of a more active variant of IL-13 (R130Q) that has reduced affinity for IL-13Rα2. Human subjects carrying R130Q reported a

Correspondence should be addressed to Kevin M. Vannella; National Institutes of Health, National Institute of Allergy and Infectious Diseases, Building 10, Room 4D12, Bethesda, MD 20814; kevin.vannella@nih.gov; phone: 301-594-2121.

Author Contributions. E.P.K., T.A.W., and K.M.V. conceived and designed the experiments; E.P.K., T.S.P., T.R.R., R.W.T., K.J.K., T.A.P., R.d.Q.P., and K.M.V. performed the experiments; E.P.K., T.S.P., T.R.R., R.W.T., R.L.G., K.J.K., A.K., D.A.H, 23andMe.R.T., T.A.P., R.d.Q.P., and N.B. analyzed the data; M.H., M.F., F.J., L.T. and M.T.K., provided reagents; E.P.K., T.A.W., and K.M.V. wrote the manuscript.

Disclosures: R.L. Gieseck III, M. Hegen, M. Farmer, F. Jin, R. de Queiroz Prado, N. Bing, L. Tchistiakova, M.T. Kasaian, and T.A. Wynn are employees of Pfizer Inc. A. Kleinman, D.A. Hinds, and the 23andMeResearch Team are employees of 23andMe. All other authors have no disclosures.

lower risk for Crohn's disease. Our findings endorse moving anti-IL-13Rα2 into preclinical drug development with the goal of accelerating recovery and maintaining remission in Crohn's disease patients.

Introduction

Crohn's disease (CD) and ulcerative colitis (UC) are inflammatory bowel diseases (IBD) usually characterized by periods of exacerbation and remission [1,2]. IBD pathogenesis has been attributed to multiple factors including genetic predispositions, microbial dysbiosis, excessive innate and adaptive immune responses, and breakdown of epithelial barrier function. A common treatment option for patients suffering from IBD is the administration of anti-tumor necrosis factor alpha (TNFα) agents; however, up to 40% of patients with active IBD do not respond to this treatment for unknown reasons [3]. Thus, further exploration of the mechanisms that underlie IBD pathogenesis is necessary to develop improved therapies.

Previous studies identified elevated transcripts of *IL13RA2* mRNA in mucosal biopsies of patients with active UC and CD who were non-responders to anti-TNFα compared to responders [4, 5]. The immunology literature to date largely indicates that IL-13Rα2 is a non-signaling decoy receptor for interleukin (IL)-13 that does not exhibit canonical JAK-STAT signaling activity[6–14]. There are a few reports that IL-13Rα2 can alternatively signal through activator protein-1, but in which contexts this happens remains controversial [15, 16]. It is widely accepted that IL-13 signaling occurs through the IL-4Rα/IL-13Rα1 heterodimer to promote type 2 immunity and that IL-13 signaling induces IL-13Rα2 expression [7, 17, 18]. IL-13Rα2 binds IL-13 with an affinity >400 fold higher than IL-4Rα/IL-13Rα1[18]. As a result, IL-13Rα2 can function as a physiological rheostat of type 2 immunity by limiting the amount of IL-13 available to drive STAT6-dependent signaling [19, 20]. Epithelial cells, fibroblasts, and smooth muscle cells of mice and humans constitutively express IL-13Rα2 [21].

As a potent type 2 cytokine, IL-13 is a critical suppressor of type 1 and type 17 inflammation associated with IBD pathogenesis [22, 23] as well as an integral promotor of wound repair[24, 25]. In spite of this, the role of IL-13 in inflammatory bowel disease is still not well understood. Although IL-13 has been reported to be an inflammatory stimulus in UC [26, 27], recent clinical studies found that anti-IL-13 therapy was not effective for UC patients[28, 29]. While IL-13 is not known to be an initial driver of CD, it has been implicated in tissue remodeling and fibrosis in CD [30, 31]. IL-13 and other type 2 cytokines are upregulated in response to tissue injury and are important for dampening inflammation and promoting wound resolution and repair[23, 32–34], requirements for recovery from both UC and CD.

We have hypothesized that the function of IL-13Rα2 as a decoy receptor for IL-13 could be detrimental in the setting of IBD by limiting the protective anti-inflammatory and prorepair functions of type 2 immunity. Previously, we have shown that the pro-inflammatory drivers of IBD, TNFα and IL-17A, can reinforce their inflammatory signal by synergizing to induce the expression of *IL13RA2* in fibroblasts *in vitro* [9]. We have also previously demonstrated

that *Il10/Il13ra2* double knockout mice were protected from piroxicam- and *Trichuris muris*-induced colitis due to the broad anti-inflammatory functions of IL-13 compensating for the absence of IL-10 [20]. This study left several important questions unanswered. First, it prompted us to test the potential of IL-13Rα2 as a therapeutic target. Second, while *IL10* and *IL10R* deficiencies are rare with few human cases published [35], the role of IL-13 and IL-13Rα2 in IBD pathogenesis remained unclear in an immunocompetent setting. Third, whether IL-13Rα2 was influential during active disease and/or recovery from IBD was unclear. Lastly, we sought data to link our findings in mice to IBD in humans.

With our new studies, we first found evidence that increased IL-13 activity is associated with protection against IBD in humans. We conducted a phenome-wide association study (PheWAS) on a common IL-13 gain-of-function variant. We show here that subjects carrying this variant had a significantly lower odds ratio for CD, but not UC. Next, we aimed to specify the role of IL-13Rα2 in an immune-competent mouse model that was amenable to studying the relapsing and remitting characteristics of CD. We chose to use a model of colitis induced by dextran sodium sulfate (DSS)[36] and followed by a recovery period. DSS causes epithelial damage that results in type 1 and type 17 immune responses, which have been associated with the pathogenesis of CD in humans[37, 38]. We also designed a neutralizing antibody against IL-13Rα2 to test IL-13Rα2 blockade as a novel therapeutic strategy during the recovery period of disease. Data from our murine model indicate that neutralizing IL-13Rα2 provides significant therapeutic benefit by diminishing type 1 and 17 inflammation and accelerating recovery by bolstering the endogenous bioactivity of IL-13.

Results

IL-13 gain-of-function variant is protective for Crohn's disease in human subjects.

The common IL-13 variant, R130Q, has increased activity compared to wild-type IL-13 [39]. R130Q has reduced affinity for IL-13Rα2, but it has a similar affinity for IL-13Rα1 as wild-type IL-13 does [40, 41]. We performed a PheWAS analysis on the 23andMe database, which contains genetic and self-reported health status information from over 600,000 subjects and evaluated the association of R130Q across a panel of immunological diseases. As expected, our results confirmed strong associations between R130Q and increased risk of allergy, asthma, and eczema (Figure 1). The same IL-13 variant has been shown to protect against psoriasis [42], and we also found this association in our PheWAS analysis. No genome-wide association between IL-13 and IBD has been reported previously. For the first time, our results revealed a significantly lower odds ratio for CD in subjects carrying R130Q (Figure 1). In contrast, we found no significant change in the odds ratio of UC in those subjects. Our PheWAS findings provide evidence that increased IL-13 activity is protective against the pathogenesis of human CD and also indicate that that protection can be antagonized by IL-13Rα2.

DSS acutely activates type 1 and type 17 pathways.

We hypothesized that IL-13Rα2 contributes to CD pathogenesis by sustaining type 1 and type 17 inflammation through its ability to diminish IL-13 signaling. To test this further, we chose a mouse model of colitis induced by DSS because the model shares many

characteristics with human CD[37, 43, 44] The pathology associated with acute DSS-induced colitis has been reported to be mediated by type 1 and type 17 immune responses that are also associated with CD[37]. We first determined whether DSS induced type 1 and type 17 inflammatory pathways in our model. DSS exposure for seven days resulted in a significant increase in the total number of leukocytes in the colonic lamina propria (Supplemental Figure 1A), which was characterized by an influx of $Ly6C^{high}MHCII^{-}$ monocytes and $CD11b^{+}Ly6G^{+}$ neutrophils into the colonic tissue compared to untreated controls (Supplemental Figures 1B and 1C). We also measured a significant increase in IFNγ^{+} and IL-17A^{+} $CD4^{+}TCR\beta^{+}$ T cells isolated from the colon following seven days of DSS administration (Supplemental Figures 1D, 1E, and 1F). In parallel with the T cell data, we measured significant increases in the protein levels of the proinflammatory cytokines TNFα, IL-12p70, IL-1β, IL-6, IFNγ, and IL-17A in colon tissue after seven days of DSS administration in wild-type mice (Supplemental Figures 2A–2F). In contrast, anti-inflammatory mediators were not increased (Supplemental Figures 2G–2J). Together, these findings support that DSS administration upregulates type 1 and 17 inflammatory mediators in the colonic tissue.

DSS-induced intestinal injury leads to increased expression of IL-13Rα2.

We have previously reported that TNFα (a type 1 inflammatory mediator) and IL-17 (a type 17 inflammatory mediator) can synergistically increase IL-13Rα2 expression in both mouse and human fibroblasts *in vitro* [9]. We next aimed to determine whether DSS induced the expression of IL-13Rα2. Wild-type mice were administered 5% DSS in drinking water for seven days (Figure 2A). IL-13Rα2 protein levels both in the colon homogenates and serum of wild-type mice administered DSS were significantly higher than those of untreated control mice (Figures 2B and 2C). We hypothesized that the type 1 and type 17 inflammatory responses were contributing to the upregulation of IL-13Rα2 *in vivo*. To test this, we neutralized TNFα, IL-17A, or both TNFα and IL-17A in wild-type mice during the seven days of DSS administration (Figure 2D). Neutralization of only TNFα or IL-17A during DSS administration did not significantly reduce the protein levels of IL-13Rα2 in either the colon or serum (Figures 2E and 2F). Neutralization of both TNFα and IL-17A significantly reduced IL-13Rα2 protein levels compared to IgG1 isotype control-treated mice. These data suggest that the pro-inflammatory mediators TNFα and IL-17A induced by DSS administration contribute to the expression of IL-13Rα2 protein *in vivo*. IL-13Rα2 levels were not decreased to levels found in naive water-treated mice, however, indicating that other mediators also can contribute to the induction of IL-13Rα2 in the absence of IL-17A and TNFα signaling.

IL-13Rα2 deficiency provides modest protection from the initiation of DSS-induced colitis.

We next investigated whether the DSS-induced IL-13Rα2 expression is contributing to disease pathogenesis. Weight-matched (Supplemental Figure 3) wild-type mice and *Il13ra2*$^{-/-}$ mice were administered 5% DSS drinking water or normal drinking water for seven days (Figure 3A). Wild-type mice lost a significant percentage of body weight compared to *Il13ra2*$^{-/-}$ mice after seven days on DSS drinking water (Figure 3B). *Il13ra2*$^{-/-}$ mice appeared markedly less hunched and scruffy compared to wild-type mice (Figure 3C). Shortening of the colon length has been widely used as a surrogate measure for increased

colon pathology in the DSS-induced colitis model [45]. As expected, wild-type mice administered DSS had significantly shorter colon lengths compared to untreated wild-type control mice (Figure 3D). Similarly, *Il13ra2*$^{-/-}$ mice administered DSS had a significant reduction in their colon lengths compared to untreated *Il13ra2*$^{-/-}$ control mice (Figure 3D). On average, wild-type mice had roughly a 26% reduction in colon length, while *Il13ra2*$^{-/-}$ mice had a 19% reduction in colon length compared to untreated controls (Figure 3E). DSS-administered wild-type and *Il13ra2*$^{-/-}$ mice both exhibited increased leukocyte infiltration, submucosal inflammation, and goblet cell depletion in the distal colon compared to untreated controls (Figure 3F), in agreement with the observed shortening in colon length. While the pathology in *Il13ra2*$^{-/-}$ mice administered DSS tended to be less severe, the differences did not reach statistical significance (Figure 3F). Although the inflammation in DSS administered *Il13ra2*$^{-/-}$ mice was not statistically different compared to wild-type controls, we measured a significant reduction in IL-17A, IL-1β, and IFNγ protein concentrations in the colon homogenates of DSS treated *Il13ra2*$^{-/-}$ mice compared to DSS administered wild-type controls (Figures 3G, 3H, and 3I). Together, these observations show that the absence of IL-13Rα2 results in modest protection from the initiation of DSS-induced colitis.

Il13ra2$^{-/-}$ mice recover faster from acute DSS-induced colitis.

Both CD and UC are relapsing and remitting inflammatory disorders. To model this in mice, we added a seven-day recovery period. Wild-type mice and *Il13ra2*$^{-/-}$ mice were administered DSS for seven days, after which all mice were placed on normal drinking water for an additional seven days (Figure 4A). *Il13ra2*$^{-/-}$ mice administered DSS lost less body weight compared to wild-type mice administered DSS mice; however, following the subsequent recovery period, no significant differences in weight loss were observed between the two groups of mice (Figure 4B). Although, *Il13ra2*$^{-/-}$ mice appeared less hunched and scruffy compared to wild-type mice (Figure 4C). Following seven days of recovery, wild-type mice administered DSS had significantly shorter colons compared to untreated wild-type controls (Figure 4D). In contrast, the colon lengths of *Il13ra2*$^{-/-}$ mice administered DSS had increased to the extent that they were not statistically different from those of untreated *Il13ra2*$^{-/-}$ mice. The average percent reduction in colon length of DSS-administered wild-type mice was nearly 15%, whereas the average percent reduction in colon length of the DSS-administered *Il13ra2*$^{-/-}$ mice was approximately 6% (Figure 4E). Following seven days of recovery, leukocyte infiltration, submucosal inflammation, and goblet cell depletion were still appreciable in the colons of wild-type mice administered DSS (Figures 4F and 4G). There were no significant differences in these measures between *Il13ra2*$^{-/-}$ mice administered DSS and untreated *Il13ra2*$^{-/-}$ mice following seven days of recovery, however (Figures 4F and 4G). Collectively, our findings demonstrate that *Il13ra2*$^{-/-}$ mice may recover faster from DSS-induced colitis. It is important to note that these data do not allow for a controlled comparison of the contributions of IL-13Rα2 during active disease and the recovery period. We address this uncertainty with studies using an anti-IL-13Rα2 antibody described later in Figure 6.

Recovery of *Il13ra2*$^{-/-}$ mice is characterized by increased type 2 immunity in the colon.

We next sought to investigate the mediators of the reduced colitis in *Il13ra2*$^{-/-}$ mice following seven days of recovery. Analogous with our histological observations, the total number of leukocytes isolated from the colonic lamina propria of *Il13ra2*$^{-/-}$ mice was significantly lower than the number isolated from wild-type mice (Figure 5A). Amongst those leukocytes, we observed an increase in both the frequency and total number of CD11b^{+}Siglec-F^{+} eosinophils in the colonic lamina propria of *Il13ra2*$^{-/-}$ mice compared to wild-type mice after seven days of recovery (Supplemental Figure 4A and Figure 5B). The frequency and total number of CD206^{+}CD163^{+} macrophages were also higher in *Il13ra2*$^{-/-}$ mice than wild-type mice (Supplemental Figure 4B and Figure 5C). In agreement with decreased overall inflammation in the colons of *Il13ra2*$^{-/-}$ mice, we measured a decreased frequency and total number of Ly6C^{high}MHCII^{-} monocytes (Supplemental Figure 4C and Figure 5D). IL-13 has also been shown to induce mucus production by goblet cells [46]. Colon sections were stained with Alcian Blue Periodic Acid Schiff (AB/PAS) to identify mucus and the staining intensity was quantitated. Again, in accordance with the predicted increase in type 2 signaling, following seven days of recovery, colon tissue from *Il13ra2*$^{-/-}$ mice exhibited significantly more AB/PAS staining than colon tissue from wild-type mice (Figure 5E).

One possible consequence of unregulated IL-13 signaling in the absence of IL-13Rα2 is the development of excessive matrix deposition or fibrosis[24]. To monitor for the development of fibrosis, colon sections from wild-type and *Il13ra2*$^{-/-}$ mice on days 0, 7, and 14 of our model were stained with Picrosirius Red (PSR), a dye that specifically binds to collagen. No significant differences in PSR quantitation were observed at any time point (Supplemental Figure 5A). Additionally, no significant changes in the gene expression of collagen genes, *Tgfb1, Tgfbr1, Thbs1,* or *Thbs4* were observed (Supplemental Figures 5B–5J). These results reveal that despite the increased type 2 immune environment in *Il13ra2*$^{-/-}$ mice, tissue healing did not result in excess scarring but rather resulted in a general decrease in pro-inflammatory cytokine-driven tissue injury.

Because we measured many parameters in the colonic tissue indicative of increased IL-13 signaling, we next aimed to identify which cell type was the source of IL-13 in the colon during recovery. After seven days of recovery, we detected a similar increase in the frequency and total number of IL-13-producing CD4^{+}TCRβ^{+} T cells in both wild-type and *Il13ra2*$^{-/-}$ mice compared to naive controls (Figure 5F). ILC2s produced some IL-13 at baseline, but the frequency and total number of IL-13^{+} ILC2s remained unchanged after DSS administration and recovery in both strains (Figure 5G).

Therapeutic blockade of IL-13Rα2 during the recovery period accelerates recovery from acute colitis pathogenesis.

While it was evident that IL-13Rα2 ablation in *Il13ra2*$^{-/-}$ mice ameliorated DSS-induced IBD, it remained unclear whether this phenotype was due to the slightly less severe induction of DSS-colitis or if IL-13Rα2 hindered recovery from DSS-induced colitis. To specifically address this, we targeted IL-13Rα2 in wild-type mice only during the recovery period. We designed a neutralizing antibody specific for murine IL-13Rα2 (Supplemental

Figure 6A) and not IL-13Rα1 (Supplemental Figure 6B) that blocks the binding of IL-13 to IL-13Rα2 (Supplemental Figures 6C and 6D). Groups of wild-type mice were administered DSS for seven days followed by seven days of recovery. On days seven and 11, groups of mice were administered anti-IL-13Rα2 or IgG1 isotype control by intraperitoneal injection (Figure 6A). Additionally, one group of mice received anti-TNFα. Lastly, one group of mice was administered a combination of anti-IL-13Rα2/anti-TNFα. Mice receiving anti-IL-13Rα2 or the anti-IL-13Rα2/anti-TNFα combination therapy rapidly gained weight after the start of therapy (Figures 6B and 6C). Mice that received anti-TNFα gradually recovered body weight, but never gained as much weight as the mice receiving anti-IL-13Rα2 or anti-IL-13Rα2/anti-TNFα. On day 14, mice were euthanized and colon lengths were measured. Mice administered anti-TNFα, anti-IL-13Rα2, or anti-IL-13Rα2/anti-TNFα had significantly longer colon lengths compared to IgG1 isotype control treated mice (Figure 6D). All three treatment groups also had significantly lower colon pathology scores compared to IgG1 isotype control-treated controls (Figure 6E). In parallel with decreased colonic inflammation, mice treated with anti-IL-13Rα2 had significantly lower colonic protein levels of TNFα, IL-6, IL-12p70, and IL-17A compared to IgG1 isotype treated control mice (Supplemental Figures 7A–7D). The pathology scores of mice treated with anti-TNFα were higher than the groups treated with anti-IL-13Rα2 or anti-IL-13Rα2/anti-TNFα. Wild-type mice administered anti-IL-13Rα2 during the recovery period of one cycle or two cycles of DSS (Supplemental Figure 8A) were not more susceptible to fibrosis than wild-type mice administered the IgG1 isotype control (Supplemental Figure 8B and 8C). Taken together, these results demonstrate that neutralizing IL-13Rα2 with an antibody only during recovery from DSS-induced colitis accelerates recovery. Furthermore, it accelerates recovery at least as well or better than anti-TNFα.

Anti-IL-13Rα2-mediated accelerated recovery is both IL-13- and eosinophil-dependent.

While we found that neutralizing IL-13Rα2 during recovery improves outcomes, it remained uncertain to what degree IL-13 was responsible for the improvement. To test this, wild-type mice that had been administered DSS were treated with anti-IL-13Rα2, anti-IL-13Rα2/anti-IL-13, or an IgG1 isotype control antibody during the recovery week (Figure 7A). Wild-type mice administered DSS and then anti-IL-13Rα2 regained body weight comparable to untreated control mice, while wild-type mice administered DSS and neutralized of IL-13 failed to regain body weight to the levels of mice that did not receive DSS (Figure 7B). Wild-type mice with neutralized IL-13 had significantly shorter colon lengths compared to mice administered only anti-IL-13Rα2 (Figure 7C). The average percent reduction in colon lengths of mice treated with IgG1, anti-IL-13Rα2, or anti-IL-13Rα2/anti-IL-13 were 22%, 11%, and 21% respectively (Figure 7D). The colon histology score of mice depleted of IL-13 were comparable to the IgG1 control groups, while the anti-IL-13Rα2 administered group had lower histology scores (Figures 7E and 7F). Together, these data confirm that the accelerated recovery from anti-IL-13Rα2 treatment is dependent on IL-13. We observed that the frequency and total number of eosinophils were higher in the colons of *Il13ra2*$^{-/-}$ mice compared to wild-type mice that did not recover as quickly from DSS-induced colitis (Figure 5B). To test if eosinophils are important for anti-IL-13Rα2-mediated recovery, we treated wild-type mice with anti-IL-13Rα2 and anti-IL-5 to deplete eosinophils during the seven day recovery period to

effectively deplete eosinophils (Supplemental Figure 9A and 9B). Wild-type mice that were depleted of eosinophils during anti-IL-13Rα2 treatment failed to improve their colon lengths unlike those with intact eosinophils (Supplemental Figure 9C). Eosinophil depletion completely eliminated the improved pathology score found in the colons of anti-IL-13Rα2 treated mice with intact eosinophils (Supplemental Figure 9D). These results demonstrate that eosinophils play a critical role in anti-IL-13Rα2-mediated recovery along with IL-13.

Discussion

Despite a number of recent studies of IL-13 in IBD, the role of IL-13 remains unclear and the findings so far indicate its role may vary in different diseases and different stages of disease. There is evidence that the character of the inflammatory response changes over the course of IBD. Type 1 and type 17 immune responses are known to be involved in the induction of CD colitis [47, 48], while type 2 cytokines have been associated with tissue remodeling and more chronic fibrotic pathology [30, 31]. Kugathasan *et al.* found that a strong type 1 immune profile exhibited by the gut mucosa of CD patients experiencing their first symptoms shifts to a more type 2 polarized milieu in patients with long-standing disease [49]. These kinetics align with established roles for IL-13 as anti-inflammatory and protissue repair[23]. In contrast, type 2 cytokines like IL-13 have been associated with the pathogenesis of UC [27, 50]. However, clinical trials of anti-IL-13 monoclonal antibodies Anrukinzumab and Tralokinumab did not show improved outcomes of patients with active UC [28, 29]. Given the varied patterns of immune pathway activation, perhaps it is not surprising that another study could not detect different levels of IL-13 production by mucosal explants and activated lamina propria mononuclear cells between CD, UC, and control subjects[51]. Collectively, the recent data indicate that immunoregulation during CD and UC is more heterogenous than simply type 1/type 17-polarized and type 2-polarized, respectively.

Analysis of immune modulation during the DSS-induced model of colitis revealed a similar pattern to the one found in early and long-term CD [37]. Type 1 and type 17 cytokines were strongly upregulated during the development of acute DSS-induced colitis, and a type 2 response was strongly upregulated later during periods of recovery from injury or during more chronic disease. These kinetics supports our hypothesis that type 2 signaling is detrimentally low when type 1 and type 17 inflammation drives DSS-induced colitis and human CD. The findings also suggest that IL-13Rα2 neutralization may be most effective during recovery because IL-13 is more highly expressed during that period.

Wang *et at.* have also demonstrated that the IL-13 that is expressed during active DSS-induced colitis does mitigate disease [52]. They found IL-13-deficient mice to be moderately more susceptible to DSS-induced colitis at least in part due to increased type 1 and type 17 cytokines. This result parallels our observation that ablating IL-13Rα2 during active disease further mitigates disease, albeit moderately, by incrementally increasing IL-13 signaling above the amount found in wild-type mice. It is important to note that IL-13 is not protective in all settings, however. Targeting IL-13 reduced the severity of murine oxazolone-induced colitis, a model that more closely resembles UC [26, 53]. Mice overexpressing GATA-3 and type 2 cytokines exhibited worse disease in a DSS-colitis model[54, 55]. These findings emphasize that too much type 2 inflammation is also detrimental and that balancing IL-13

and type 2 immunity is essential for managing IBD. As we show in our model, exploiting the ability of IL-13Rα2 to be a rheostat for IL-13 provides a powerful therapeutic tool. Achieving the best outcomes requires finding the right balance of type 1, type 17, and type 2 immune responses.

Elevated expression of *IL13RA2* has been previously identified in patients suffering from IBD, and its expression is highly upregulated in patients who do not respond to the current standard therapy, anti-TNFα [4, 5]. IL-13Rα2 has yet to be tested as a therapeutic target and questions remained about how and when IL-13Rα2 promotes IBD. Using a murine model of DSS-induced colitis, we provide evidence that IL-13Rα2 slows the recovery from IBD by limiting the anti-inflammatory functions of IL-13. We also find that therapeutic neutralization of IL-13Rα2 using a novel anti-IL-13Rα2 mAb accelerates recovery from DSS-induced colitis and demonstrate that enhanced IL-13-mediated signaling is responsible for the improvement.

The DSS-induced model has been well characterized [43]. We preferred it to other murine models for several reasons. First, it can be used in immunocompetent mice. Second, its acute pro-inflammatory immune profile is consistent with that found in CD [37]. Third, while it causes inflammation limited to the colon similarly to human UC, the inflammation is transmural similar to CD [44]. Lastly, by taking the mice off of DSS and administering water for a period, we could model the injury and recovery periods seen in human disease. This allowed us to interrogate the role of IL-13Rα2 during both periods of disease.

The initiation of DSS-induced colitis is characterized by robust production of type 1 and type 17 pro-inflammatory mediators [37] which we have previously shown induce the expression of IL-13Rα2 *in vitro*[9]. We demonstrated that administration of drinking water with 5% DSS induces production of colonic and systemic IL-13Rα2 protein. The increased murine IL-13Rα2 production is consistent with human data showing increased expression of *IL13RA2* in inflamed colon tissue of IBD patients [4, 5]. We found that the upregulation of IL-13Rα2 following seven days of DSS administration is at least partly dependent on type 1 and type 17 mediators as neutralization of TNFα and IL-17A significantly reduced the protein concentrations of both colonic and systemic IL-13Rα2. Neutralization of TNFα and IL-17A did not reduce IL-13Rα2 to levels found in naïve controls, suggesting that other pro-inflammatory mediators induce IL-13Rα2 production in the absence of TNFα and IL-17A signaling during inflammation *in vivo.* Neutralizing TNFα alone did not reduce colonic or serum IL-13Rα2 protein levels. This suggests that repair and recovery that we observed in the colons of mice administered anti-TNFα/anti-IL-13Rα2 is due to the increased activity of IL-13 when IL-13Rα2 is neutralized, rather than anti-TNFα reducing the amount of IL-13Rα2 protein in the colon.

We next aimed to investigate the role of IL-13Rα2 in DSS-induced colitis. While both *Il13ra2*$^{-/-}$ and wild-type mice administered DSS had a significant reduction in their colon lengths and extensive colonic inflammation, mice in which IL-13Rα2 was ablated were modestly protected from disease induction compared to wild-type controls. *Il13ra2*$^{-/-}$ mice showed significantly accelerated improvement when an additional seven-day recovery period was added, suggesting that IL-13Rα2 plays a prominent role in recovery after tissue

injury. Another recently published study also drew this conclusion[56]. Verstockt *et al.* found that IL-13Rα2 ablation did not significantly ameliorate pathology during the induction of colitis by DSS. Three days after removing DSS, *Il13ra2*$^{-/-}$ mice observed decreased inflammation and promoted goblet cell regeneration [56]. While these findings suggested that IL-13Rα2 ablation was more effective during recovery than active disease, they did not allow for a controlled comparison of the respective contributions of IL-13Rα2 during active disease and recovery. To address this, we neutralized IL-13Rα2 with an antibody during only the recovery phase. The results confirmed that IL-13Rα2 neutralization promotes tissue recovery. Our data supports that abrogating IL-13Rα2 during the induction period of DSS-induced colitis is less effective at preventing the severity of colitis because of the low levels of IL-13 that are induced compared to untreated control mice. Previous studies of the immune kinetics of DSS-induced colitis and human CD have demonstrated that the immune response shifts from that pro-inflammatory milieu during pathogenesis towards an anti-inflammatory and pro-wound healing milieu [37, 49]. This is likely particularly true after DSS is removed and severe tissue injury has already occurred. In this environment, type 2 cytokines like IL-13 potently contribute to tissue remodeling [23, 32–34, 37].

We also investigated the mechanisms which contributed to the decreased colonic inflammation in *Il13ra2*$^{-/-}$ mice. We observed many parameters indicative of increased IL-13 activity, including increased mucus production in colon tissue of *Il13ra2*$^{-/-}$ mice compared to wild-type mice after the recovery period. Eosinophils have been shown to be both pathogenic and protective in the induction of DSS-induced colitis [57, 58]. We identified an increase in the frequency and total number of eosinophils in the rapidly recovering colons of *Il13ra2*$^{-/-}$ mice. In this setting, eosinophils can suppress type 1 and type 17 inflammation by polarizing T cells towards a TH_2 phenotype, reducing neutrophilia, boosting immune tolerance and secreting IL-13 [58–60]. Additionally, eosinophils have been shown to have a pro-regenerative function following liver injury and play an anti-inflammatory role in a mouse model of arthritis [51, 61, 62]. Our findings support a critical repair function of eosinophils during the recovery from DSS-induced colitis, as mice depleted of eosinophils specifically during anti-IL-13Rα2-mediated recovery failed to resolve colonic inflammation. Eosinophils can suppress type 1 inflammatory responses, restrict bacteria-induced gut inflammation [63], and stimulate fibrogenic progenitors to promote muscle regeneration [64]. We also identified elevated frequency and total numbers of macrophages expressing both CD206 and CD163. CD206 and CD163 are scavenger receptors for mannose found on the surface of microorganisms and hemoglobin-haptoglobin complexes, respectively [65, 66]. The upregulation of scavenger receptors specific for inflammatory stimuli correlates with decreased inflammation in and quicker recovery observed in the *Il13ra2*$^{-/-}$ mice.

To date, genome-wide association studies (GWAS) have associated many genetic loci with IBD [67]; however, the association of IL-13 with IBD at genome-wide significance has not been reported. The R130Q IL-13 gain-of-function variant has reduced affinity for IL-13Rα2 because of the substitution of a glutamine residue at position 130 located in the D α-helix [39]. Alanine scanning experiments have demonstrated that this substitution is important for IL-13 binding to IL-13Rα2 [68]. R130Q is also the causal variant for positive associations with asthma and psoriasis. We rationalized that the R130Q IL-13 served as the best genetic tool to analyze the association of IL-13 and IL-13Rα2 with IBD. Increased IL-13 activity in human

subjects had no association with the occurrence of UC. We found this surprising given the previous reports connecting IL-13 with UC pathogenesis. As we discussed above, however, anti-IL-13 therapy recently failed to improve outcomes in a clinical trial of UC patients. The size of our PheWAS cohort adds to the mounting evidence that the pathogenesis of UC may be more immunologically heterogenous than originally thought. On the other hand, our PheWAS analysis provided perhaps the strongest evidence to date that increased IL-13 activity is protective against CD pathogenesis. R130Q likely has a greater propensity to downregulate type 1 and type 17 inflammation and promote tissue remodeling because less of it is bound to IL-13Rα2 than unmutated IL-13. Our PheWAS findings also support our observations in mice. In both cases, increased IL-13 activity is protective against colitis resembling CD.

Our final experiments were intended to confirm that IL-13 activity was also responsible for the therapeutic effects in the mouse model. In contrast to the rapid recovery observed in animals treated with anti-IL-13Rα2, mice treated with anti-IL-13Rα2 in combination with anti-IL-13 to neutralize IL-13 during the recovery period failed to regain their body weight and had comparable colon lengths and colonic inflammation as IgG1 isotype control treated mice. These findings also provide strong evidence that targeting IL-13 as a therapy for CD could be problematic. In contrast, the data show that IL-13 plays a protective role by promoting broad anti-inflammatory activity during the recovery period.

In this study, we provide compelling evidence that the increased production of IL-13Rα2 during type 1/type 17 colitis plays a pathogenic role by impeding IL-13-mediated recovery. Our results argue that targeting IL-13Rα2 to bolster endogenous IL-13 bioactivity could represent a highly efficacious therapy to promote resolution of IBD-mediated damage and may be especially useful as an alternative therapy for patients who have failed or developed resistance to anti-TNFα agents.

Methods

Human Subjects.

All research participants included in the phenome-wide association analyses provided informed consent and answered surveys online according to 23andMe's human subjects protocol, which was reviewed and approved by Ethical & Independent Review Services, a private institutional review board (http://www.eandireview.com).

Phenome-Wide Association Study.

A phenome-wide association analysis of the European 23andMe cohort of the SNP, rs20541, the genetic polymorphism of the IL-13 R130Q variant, was performed. The association was conducted for disease case control endpoints via logistic regression, assuming additive allelic effects, and included covariates for age, gender, and the top four principal components to account for residual population structure. The association test *p*-value we report was computed using a likelihood ratio test.

Mice.

Age and weight-matched female wild-type and *Il13ra2*$^{-/-}$ mice on a BALB/c genetic background between the ages of 8-12 weeks were used in experiments and purchased from Taconic Biosciences. Some studies were repeated in males to confirm there were no gender biases. Mice were housed under specific pathogen-free conditions at the National Institutes of Health in an Association for Assessment and Accreditation of Laboratory Animal Care approved facility. The National Institute of Allergy and Infectious Diseases Animal Care and Use Committee approved all experimental procedures.

DSS-induced Colitis.

Acute colitis was induced by 5% (w/v) dextran sodium sulfate (DSS; MW 40,000-50,000 Da; Alfa Aesar) added to drinking water. The 5% dose of DSS was chosen based on the genetic background of the mice used in our studies, and the cleanliness of our housing facility. Mice were left on DSS water for seven days and then were placed on normal drinking water for seven days. Colitis severity was determined by measuring body weight and colon length. Alternatively, mice were subjected to 5% DSS drinking water for seven days, followed by seven days on normal drinking water for two cycles.

Antibody Administration.

Mice were injected intraperitoneally with 250μg/mouse of anti-IL-17A (17F3), anti-TNFα (XT22.11), or IgG1 isotype control (MOPC-21) on days zero and four. For studies where antibodies were administered during the recovery, mice were injected intraperitoneally with 250μg/mouse of anti-IL-13Rα2 (6D5), anti-TNFα (XT22.11), anti-IL-13Rα2 (6D5)/anti-TNFα (XT22.11), anti-IL-13Rα2 (6D5)/anti-IL-13 (262A-5-1), anti-IL-13Rα2 (6D5)/anti-IL-5 (TRFK5) or IgG1 isotype control (HPRN) on day seven, 11, 21, or 25.

Physical Appearance.

For physical appearance, mice were scored on the following 3-point scale: 0 is equal to normal; 1 is a scruffy appearance; 2 is a scruffy and hunched appearance; 3 is a scruffy, hunched appearance with no motility.

Histopathology.

For histopathological analysis, distal colons were flushed with 1X phosphate-buffered saline and a 6mm piece of distal colon was harvested, fixed in 10% phosphate-buffered formalin, and embedded in paraffin. 5-μm sections were cut and stained with Hematoxylin and Eosin (H&E), Picrosirius Red (PSR) and counterstained with fast green, or Alacian Blue Periodic Acid-Schiff (ABPAS). Sections were scored by a blinded scorer based on goblet cell depletion, leukocyte infiltration, and submucosal inflammation on a point scale of 0-3, where 0 is no pathology and 3 is most severe pathology.

Histological Quantification.

Slides stained with ABPAS or PSR with fast green counterstain were digitized using an Aperio Scanscope® CS system. The percentage of total area positive for ABPAS or PSR

was quantitated using the Aperio ImageScope Positive Pixel Count v9 algorithm. Positive pixel area percentages were exported to GraphPad Prism 7 for statistical analyses.

Colon Lysates.

Pre-weighed colons were placed into a Precellys tubes containing 500μL radioimmunoprecipitation assay buffer with protease inhibitor. Tissues were homogenized using a Precellys homogenizer and centrifuged at 10,000 RPM for 10 minutes at 4°C. Colon lysate supernatants were frozen at −80°C until used.

IL-13Rα2 ELISA.

Colonic and systemic IL-13Rα2 protein concentrations were determined by ELISA assay as previously described [69]. High protein binding 96-well plates were coated with anti-IL-13Rα2 (1μg/mL; R&D) in PBS overnight and a biotinylated anti-mouse IL-13 (2μg/mL; Centocor) was used for detection.

Luminex Analysis of Cytokine Expression.

TNFα, IL-12p70, IL-1β, IL-6, IFNγ, IL-17A, IL-13, IL-4, IL-10, and IL-5 cytokine concentrations in the colon homogenates were determined using an enzyme-linked immunosorbent assay using the MILLIPLEX MAP Mouse TH17 Magnetic Bead Panel (Millipore Sigma) according to the manufacture's protocol. Analytes were read using a Bio-Rad Bio-Plex 200 system. Concentrations of cytokines were determined by standard curve using recombinant proteins.

RNA Capture and Purification.

Colons were harvested and placed in a Precellys tube containing 500μL Trizol. Tissues were then homogenized using a Precellys homogenizer. RNA capture and purification were performed using MagMAX-96 Total RNA Isolation Kit (Thermo Fisher). RNA concentration (ng/μL) was determined using a DeNovix DS-11 Spectrophotometer.

RNA Expression Profiling.

Preparation, hybridization, and detection of RNA samples were carried out by following Nanostring manufacturer's instructions (Nanostring Technologies). Subsequent analyses were performed using nCounter Analysis System and TM4 MeV microarray software suite.

Isolation of Colonic Lamina Propria Leukocytes.

Murine colonic lamina propria leukocytes were isolated as previously described [70].

Intracellular Cytokine Staining.

Lymphocytes isolated from the colonic lamina propria were restimulated *ex vivo* with PMA (50ng/mL) and lonomycin (500ng/mL) in the presence of Brefeldin A for 3 hours at 37°C. Cells were then stained with fluorescently labeled antibodies for surface antigens, followed by permeabilization with Cytofix/Cytoperm (BD), and stained for intracellular cytokines in Perm/Wash (BD).

Antibodies and FACS Analysis.

Fluorescently labelled antibodies purchased from eBioscience (Waltham, MA) include the following: TCRβ (biotin; 1:200), TCRγδ (biotin; 1:200), and CD19 (biotin; 1:200), TCRβ (H57-597; 1:200), CD19 (eBio1D3; 1:200), TCRγδ (EbioGL3; 1:200), CD45.2 (104; 1:400), CD163 (TNKUPJ; 1:100) and IFNγ (XMG1.2; 1:100). Antibodies purchased from Biolegend (San Diego, CA) include the following: CD16/CD32 (93; 1:500), Streptavidin, CD11b(M1/70; 1:500), F4/80 (BM8; 1:200), CD206 (C068C2; 1:200), and IL-17A (TC11-18H10.1, 1:100). Antibodies purchased from BD Pharmingen (Billerica, MA) include the following: Siglec-F (E50-2440; 1:800), CD64 (X54-5/7.1; 1:200) and CD4 (RM4.5; 1:200). Antibodies purchased from Life Technologies (Washington, DC) include the following: LIVE/DEAD Fixable Blue Viability Dye (1:500). Cells were collected on an LSR Fortessa I flow cytometer equipped with FACSDIVA (BD Biosciences) software and data were analyzed with FlowJo software (Tree Star, Ashland, OR).

Statistical Analysis.

Experimental results are represented as mean +/− standard error or geometric mean. Statistical differences were determined by using Mann-Whitney, two-tailed student T-test, or One-way ANOVA. For both statistical tests, a p value of <0.05 was deemed statistically significant. Graphing and statistical analysis were performed using GraphPad Prism 7 software. *p<0.05, **p<0.01, ***p<0.001, and ****p<0.0001; ns denotes not significant. Data are pooled from 2-3 independent experiments.

Supplementary Material

Refer to Web version on PubMed Central for supplementary material.

Acknowledgements.

This project was funded and supported by the Intramural Research Program of the National Institutes of Health, National Institute of Allergy and Infectious Diseases and Pfizer Inc. We would like to thank Elizabeth A. Connor and the CCR Genomics Core for assistance with Nanostring. We would also like to thank Patrick Lin, Sandra White, and Kevin Hart for assistance with animal work and thoughtful scientific discussion. We thank Ginger Chen for assistance with IL-13Rα2 K_D experiments. Lastly, we thank the National Institute of Allergy and Infectious Diseases Veterinary Services team for animal care and weighing mice throughout the studies. Erik P. Karmele is a predoctoral student in The George Washington University-National Institutes of Health Graduate Partnerships Program. This work is presented to the above program in partial fulfillment of the requirements for the Ph.D. degree.

Grant Support: This project was funded and supported by the Intramural Research Program of the National Institutes of Health, National Institute of Allergy and Infectious Diseases and Pfizer Inc.

References

1. Lee JM, Lee KM. Endoscopic Diagnosis and Differentiation of Inflammatory Bowel Disease. Clin Endosc 2016; 49(4): 370–375. [PubMed: 27484813]
2. Loftus EV Jr. Clinical epidemiology of inflammatory bowel disease: Incidence, prevalence, and environmental influences. Gastroenterology 2004; 126(6): 1504–1517. [PubMed: 15168363]
3. Rubbert-Roth A, Finckh A. Treatment options in patients with rheumatoid arthritis failing initial TNF inhibitor therapy: a critical review. Arthritis Res Ther 2009; 11 Suppl 1: S1. [PubMed: 19368701]

4. Arijs I, Li K, Toedter G, Quintens R, Van Lommel L, Van Steen K et al. Mucosal gene signatures to predict response to infliximab in patients with ulcerative colitis. Gut 2009; 58(12): 1612–1619. [PubMed: 19700435]
5. Arijs I, Quintens R, Van Lommel L, Van Steen K, De Hertogh G, Lemaire K et al. Predictive value of epithelial gene expression profiles for response to infliximab in Crohn's disease. Inflamm Bowel Dis 2010; 16(12): 2090–2098. [PubMed: 20848504]
6. Lupardus PJ, Birnbaum ME, Garcia KC. Molecular basis for shared cytokine recognition revealed in the structure of an unusually high affinity complex between IL-13 and IL-13Ralpha2. Structure 2010; 18(3): 332–342. [PubMed: 20223216]
7. Chandriani S, DePianto DJ, N'Diaye EN, Abbas AR, Jackman J, Bevers J 3rd et al. Endogenously expressed IL-13Ralpha2 attenuates IL-13-mediated responses but does not activate signaling in human lung fibroblasts. J Immunol 2014; 193(1): 111–119. [PubMed: 24879793]
8. Kawakami K, Taguchi J, Murata T, Puri RK. The interleukin-13 receptor alpha2 chain: an essential component for binding and internalization but not for interleukin-13-induced signal transduction through the STAT6 pathway. Blood 2001; 97(9): 2673–2679. [PubMed: 11313257]
9. Badalyan V, Thompson R, Addo K, Borthwick LA, Fisher AJ, Ort T et al. TNF-alpha/IL-17 synergy inhibits IL-13 bioactivity via IL-13Ralpha2 induction. J Allergy Clin Immunol 2014; 134(4): 975–978 e975. [PubMed: 24954262]
10. Yasunaga S, Yuyama N, Arima K, Tanaka H, Toda S, Maeda M et al. The negative-feedback regulation of the IL-13 signal by the IL-13 receptor alpha2 chain in bronchial epithelial cells. Cytokine 2003; 24(6): 293–303. [PubMed: 14609571]
11. Mentink-Kane MM, Wynn TA. Opposing roles for IL-13 and IL-13 receptor alpha 2 in health and disease. Immunol Rev 2004; 202: 191–202. [PubMed: 15546394]
12. Chiaramonte MG, Mentink-Kane M, Jacobson BA, Cheever AW, Whitters MJ, Goad ME et al. Regulation and function of the interleukin 13 receptor alpha 2 during a T helper cell type 2-dominant immune response. J Exp Med2003; 197(6): 687–701. [PubMed: 12642601]
13. Andrews AL, Nasir T, Bucchieri F, Holloway JW, Holgate ST, Davies DE. IL-13 receptor alpha 2: a regulator of IL-13 and IL-4 signal transduction in primary human fibroblasts. J Allergy Clin Immunol 2006; 118(4): 858–865. [PubMed: 17030238]
14. Feng N, Lugli SM, Schnyder B, Gauchat JF, Graber P, Schlagenhauf E et al. The interleukin-4/interleukin-13 receptor of human synovial fibroblasts: overexpression of the nonsignaling interleukin-13 receptor alpha2. Lab Invest 1998; 78(5): 591–602. [PubMed: 9605184]
15. Fichtner-Feigl S, Strober W, Kawakami K, Puri RK, Kitani A. IL-13 signaling through the IL-13alpha2 receptor is involved in induction of TGF-beta1 production and fibrosis. Nat Med 2006; 12(1): 99–106. [PubMed: 16327802]
16. Rahaman SO, Vogelbaum MA, Haque SJ. Aberrant Stat3 signaling by interleukin-4 in malignant glioma cells: involvement of IL-13Ralpha2. Cancer Res 2005; 65(7): 2956–2963. [PubMed: 15805299]
17. Wynn TA. IL-13 effector functions. Annu Rev Immunol 2003; 21: 425–456. [PubMed: 12615888]
18. Andrews AL, Holloway JW, Puddicombe SM, Holgate ST, Davies DE. Kinetic analysis of the interleukin-13 receptor complex. J Biol Chem 2002; 277(48): 46073–46078. [PubMed: 12354755]
19. Wilson MS, Elnekave E, Mentink-Kane MM, Hodges MG, Pesce JT, Ramalingam TR et al. IL-13Ralpha2 and IL-10 coordinately suppress airway inflammation, airway-hyperreactivity, and fibrosis in mice. J Clin Invest 2007; 117(10): 2941–2951. [PubMed: 17885690]
20. Wilson MS, Ramalingam TR, Rivollier A, Shenderov K, Mentink-Kane MM, Madala SK et al. Colitis and intestinal inflammation in IL10−/− mice results from IL-13Ralpha2-mediated attenuation of IL-13 activity. Gastroenterology 2011; 140(1): 254–264. [PubMed: 20951137]
21. Tabata Y, Khurana Hershey GK. IL-13 receptor isoforms: breaking through the complexity. Curr Allergy Asthma Rep 2007; 7(5): 338–345. [PubMed: 17697639]
22. Abbas AK, Murphy KM, Sher A. Functional diversity of helper T lymphocytes. Nature 1996; 383(6603): 787–793. [PubMed: 8893001]
23. Wynn TA. Type 2 cytokines: mechanisms and therapeutic strategies. Nat Rev Immunol 2015; 15(5): 271–282. [PubMed: 25882242]

24. Gieseck RL 3rd, Ramalingam TR, Hart KM, Vannella KM, Cantu DA, Lu WY et al. Interleukin-13 Activates Distinct Cellular Pathways Leading to Ductular Reaction, Steatosis, and Fibrosis. Immunity 2016; 45(1): 145–158. [PubMed: 27421703]
25. Gieseck RL 3rd, Wilson MS, Wynn TA. Type 2 immunity in tissue repair and fibrosis. Nat Rev Immunol 2018; 18(1): 62–76. [PubMed: 28853443]
26. Heller F, Fuss IJ, Nieuwenhuis EE, Blumberg RS, Strober W. Oxazolone colitis, a Th2 colitis model resembling ulcerative colitis, is mediated by IL-13-producing NK-T cells. Immunity 2002; 17(5): 629–638. [PubMed: 12433369]
27. Fuss IJ, Heller F, Boirivant M, Leon F, Yoshida M, Fichtner-Feigl S et al. Nonclassical CD1d-restricted NK T cells that produce IL-13 characterize an atypical Th2 response in ulcerative colitis. J Clin Invest 2004; 113(10): 1490–1497. [PubMed: 15146247]
28. Reinisch W, Panes J, Khurana S, Toth G, Hua F, Comer GM et al. Anrukinzumab, an anti-interleukin 13 monoclonal antibody, in active UC: efficacy and safety from a phase IIa randomised multicentre study. Gut 2015; 64(6): 894–900. [PubMed: 25567115]
29. Danese S, Rudzinski J, Brandt W, Dupas JL, Peyrin-Biroulet L, Bouhnik Y et al. Tralokinumab for moderate-to-severe UC: a randomised, double-blind, placebo-controlled, phase IIa study. Gut 2015; 64(2): 243–249. [PubMed: 25304132]
30. Scharl M, Frei S, Pesch T, Kellermeier S, Arikkat J, Frei P et al. Interleukin-13 and transforming growth factor beta synergise in the pathogenesis of human intestinal fistulae. Gut 2013; 62(1): 63–72. [PubMed: 22287592]
31. Curciarello R, Docena GH, MacDonald TT. The Role of Cytokines in the Fibrotic Responses in Crohn's Disease. Front Med (Lausanne) 2017; 4: 126. [PubMed: 28824915]
32. Dalessandri T, Crawford G, Hayes M, Castro Seoane R, Strid J. IL-13 from intraepithelial lymphocytes regulates tissue homeostasis and protects against carcinogenesis in the skin. Nat Commun 2016; 7: 12080. [PubMed: 27357235]
33. Bosurgi L, Cao YG, Cabeza-Cabrerizo M, Tucci A, Hughes LD, Kong Y et al. Macrophage function in tissue repair and remodeling requires IL-4 or IL-13 with apoptotic cells. Science 2017; 356(6342): 1072–1076. [PubMed: 28495875]
34. Gause WC, Wynn TA, Allen JE. Type 2 immunity and wound healing: evolutionary refinement of adaptive immunity by helminths. Nat Rev Immunol 2013; 13(8): 607–614. [PubMed: 23827958]
35. Glocker EO, Kotlarz D, Boztug K, Gertz EM, Schaffer AA, Noyan F et al. Inflammatory bowel disease and mutations affecting the interleukin-10 receptor. N Engl J Med 2009; 361(21): 2033–2045. [PubMed: 19890111]
36. Okayasu I, Hatakeyama S, Yamada M, Ohkusa T, Inagaki Y, Nakaya R. A novel method in the induction of reliable experimental acute and chronic ulcerative colitis in mice. Gastroenterology 1990; 98(3): 694–702. [PubMed: 1688816]
37. Alex P, Zachos NC, Nguyen T, Gonzales L, Chen TE, Conklin LS et al. Distinct cytokine patterns identified from multiplex profiles of murine DSS and TNBS-induced colitis. Inflamm Bowel Dis 2009; 15(3): 341–352. [PubMed: 18942757]
38. Siakavellas SI, Bamias G. Role of the IL-23/IL-17 axis in Crohn's disease. Discov Med 2012; 14(77): 253–262. [PubMed: 23114581]
39. Vladich FD, Brazille SM, Stern D, Peck ML, Ghittoni R, Vercelli D. IL-13 R130Q, a common variant associated with allergy and asthma, enhances effector mechanisms essential for human allergic inflammation. J Clin Invest 2005; 115(3): 747–754. [PubMed: 15711639]
40. Yoshida Y, Ohkuri T, Takeda C, Kuroki R, Izuhara K, Imoto T et al. Analysis of internal motions of interleukin-13 variant associated with severe bronchial asthma using (15)N NMR relaxation measurements. Biochem Biophys Res Commun 2007; 358(1): 292–297. [PubMed: 17482144]
41. Lacy ER. Equilibrium and kinetic analysis of human interleukin-13 and IL-13 receptor alpha-2 complex formation. J Mol Recognit 2012; 25(3): 184–191. [PubMed: 22407982]
42. Lee YH, Choi SJ, Ji JD, Song GG. Genome-wide pathway analysis of a genomewide association study on psoriasis and Behcet's disease. Mol Biol Rep 2012; 39(5): 5953–5959. [PubMed: 22201026]

43. Wirtz S, Popp V, Kindermann M, Gerlach K, Weigmann B, Fichtner-Feigl S et al. Chemically induced mouse models of acute and chronic intestinal inflammation. Nat Protoc 2017; 12(7): 1295–1309. [PubMed: 28569761]
44. Melgar S, Karlsson L, Rehnstrom E, Karlsson A, Utkovic H, Jansson L et al. Validation of murine dextran sulfate sodium-induced colitis using four therapeutic agents for human inflammatory bowel disease. Int Immunopharmacol 2008; 8(6): 836–844. [PubMed: 18442787]
45. Chassaing B, Aitken JD, Malleshappa M, Vijay-Kumar M. Dextran sulfate sodium (DSS)-induced colitis in mice. Curr Protoc Immunol 2014; 104: Unit 15 25.
46. Birchenough GM, Johansson ME, Gustafsson JK, Bergstrom JH, Hansson GC. New developments in goblet cell mucus secretion and function. Mucosal Immunol 2015; 8(4): 712–719. [PubMed: 25872481]
47. Fuss IJ, Neurath M, Boirivant M, Klein JS, de la Motte C, Strong SA et al. Disparate CD4+ lamina propria (LP) lymphokine secretion profiles in inflammatory bowel disease. Crohn's disease LP cells manifest increased secretion of IFN-gamma, whereas ulcerative colitis LP cells manifest increased secretion of IL-5. J Immunol 1996; 157(3): 1261–1270. [PubMed: 8757634]
48. Fujino S, Andoh A, Bamba S, Ogawa A, Hata K, Araki Y et al. Increased expression of interleukin 17 in inflammatory bowel disease. Gut 2003; 52(1): 65–70. [PubMed: 12477762]
49. Kugathasan S, Saubermann LJ, Smith L, Kou D, Itoh J, Binion DG et al. Mucosal T-cell immunoregulation varies in early and late inflammatory bowel disease. Gut 2007; 56(12): 1696–1705. [PubMed: 17682002]
50. Heller F, Florian P, Bojarski C, Richter J, Christ M, Hillenbrand B et al. Interleukin-13 is the key effector Th2 cytokine in ulcerative colitis that affects epithelial tight junctions, apoptosis, and cell restitution. Gastroenterology 2005; 129(2): 550–564. [PubMed: 16083712]
51. Biancheri P, Di Sabatino A, Ammoscato F, Facciotti F, Caprioli F, Curciarello R et al. Absence of a role for interleukin-13 in inflammatory bowel disease. Eur J Immunol 2014; 44(2): 370–385. [PubMed: 24338958]
52. Wang AJ, Smith A, Li Y, Urban JF Jr., Ramalingam TR, Wynn TA et al. Genetic deletion of IL-25 (IL-17E) confers resistance to dextran sulfate sodium-induced colitis in mice. Cell Biosci 2014; 4: 72. [PubMed: 25937893]
53. Kasaian MT, Page KM, Fish S, Brennan A, Cook TA, Moreira K et al. Therapeutic activity of an interleukin-4/interleukin-13 dual antagonist on oxazolone-induced colitis in mice. Immunology 2014; 143(3): 416–427. [PubMed: 24831554]
54. Okamura M, Yoh K, Ojima M, Morito N, Takahashi S. Overexpression of GATA-3 in T cells accelerates dextran sulfate sodium-induced colitis. Exp Anim 2014; 63(2): 133–140. [PubMed: 24770638]
55. Zhu J, Yang F, Sang L, Zhai J, Zhang X, Yue D et al. IL-33 Aggravates DSS-Induced Acute Colitis in Mouse Colon Lamina Propria by Enhancing Th2 Cell Responses. Mediators Inflamm 2015; 2015: 913041. [PubMed: 26161006]
56. Verstockt B, Perrier C, De Hertogh G, Cremer J, Creyns B, Van Assche G et al. Effects of Epithelial IL-13Rα2 Expression in Inflammatory Bowel Disease. 2018; 9(2983).
57. Ahrens R, Waddell A, Seidu L, Blanchard C, Carey R, Forbes E et al. Intestinal macrophage/epithelial cell-derived CCL11/eotaxin-1 mediates eosinophil recruitment and function in pediatric ulcerative colitis. J Immunol 2008; 181(10): 7390–7399. [PubMed: 18981162]
58. Masterson JC, McNamee EN, Fillon SA, Hosford L, Harris R, Fernando SD et al. Eosinophil-mediated signalling attenuates inflammatory responses in experimental colitis. Gut 2015; 64(8): 1236–1247. [PubMed: 25209655]
59. Jacobsen EA, Ochkur SI, Pero RS, Taranova AG, Protheroe CA, Colbert DC et al. Allergic pulmonary inflammation in mice is dependent on eosinophil-induced recruitment of effector T cells. J Exp Med 2008; 205(3): 699–710. [PubMed: 18316417]
60. Odemuyiwa SO, Ghahary A, Li Y, Puttagunta L, Lee JE, Musat-Marcu S et al. Cutting edge: human eosinophils regulate T cell subset selection through indoleamine 2,3-dioxygenase. J Immunol 2004; 173(10): 5909–5913. [PubMed: 15528322]

61. Yao Y, Wang ZC, Liu JX, Ma J, Chen CL, Deng YK et al. Increased expression of TIPE2 in alternatively activated macrophages is associated with eosinophilic inflammation and disease severity in chronic rhinosinusitis with nasal polyps. Int Forum Allergy Rhinol 2017.

62. Chen Z, Andreev D, Oeser K, Krljanac B, Hueber A, Kleyer A et al. Th2 and eosinophil responses suppress inflammatory arthritis. Nat Commun 2016; 7: 11596. [PubMed: 27273006]

63. Arnold IC, Artola-Boran M, Tallon de Lara P, Kyburz A, Taube C, Ottemann K et al. Eosinophils suppress Th1 responses and restrict bacterially induced gastrointestinal inflammation. J Exp Med 2018; 215(8): 2055–2072. [PubMed: 29970473]

64. Heredia JE, Mukundan L, Chen FM, Mueller AA, Deo RC, Locksley RM et al. Type 2 innate signals stimulate fibro/adipogenic progenitors to facilitate muscle regeneration. Cell 2013; 153(2): 376–388. [PubMed: 23582327]

65. Yang H, Wang H, Levine YA, Gunasekaran MK, Wang Y, Addorisio M et al. Identification of CD163 as an antiinflammatory receptor for HMGB1-haptoglobin complexes. JCI Insight 2016; 1(7).

66. Lee SJ, Evers S, Roeder D, Parlow AF, Risteli J, Risteli L et al. Mannose receptor-mediated regulation of serum glycoprotein homeostasis. Science 2002; 295(5561): 1898–1901. [PubMed: 11884756]

67. Liu JZ, van Sommeren S, Huang H, Ng SC, Alberts R, Takahashi A et al. Association analyses identify 38 susceptibility loci for inflammatory bowel disease and highlight shared genetic risk across populations. Nat Genet 2015; 47(9): 979–986. [PubMed: 26192919]

68. Madhankumar AB, Mintz A, Debinski W. Alanine-scanning mutagenesis of alpha-helix D segment of interleukin-13 reveals new functionally important residues of the cytokine. J Biol Chem 2002; 277(45): 43194–43205. [PubMed: 12189139]

69. Zuo L, Fulkerson PC, Finkelman FD, Mingler M, Fischetti CA, Blanchard C et al. IL-13 induces esophageal remodeling and gene expression by an eosinophil-independent, IL-13R alpha 2-inhibited pathway. J Immunol 2010; 185(1): 660–669. [PubMed: 20543112]

70. Weigmann B, Tubbe I, Seidel D, Nicolaev A, Becker C, Neurath MF. Isolation and subsequent analysis of murine lamina propria mononuclear cells from colonic tissue. Nat Protoc 2007; 2(10): 2307–2311. [PubMed: 17947970]

Disease/Phenotype	Cases(n)	Controls(n)	*p*-value
Psoriatic Arthritis	3207	626849	$6x10^{-09}$
Psoriasis	38000	587061	$2x10^{-27}$
Vitiligo	4479	570081	$4x10^{-04}$
Crohn's Disease	8813	609297	$5x10^{-04}$
Any Autoimmune	108231	549784	$5x10^{-16}$
Lupus	8174	623076	$4x10^{-01}$
Ulcerative Colitis	12913	615056	$3x10^{-01}$
Celiac Disease	10255	595343	$4x10^{-01}$
Rheumatoid Arthritis	20200	606184	$3x10^{-01}$
Multiple Sclerosis	4100	626224	$1x10^{0}$
Scleroderma	1198	609571	$5x10^{-01}$
Any Allergy	240680	337684	$7x10^{-20}$
Alopecia Areata	3576	378846	$5x10^{-02}$
Any Asthma	99414	443027	$3x10^{-38}$
Eczema	78632	533760	$8x10^{-42}$

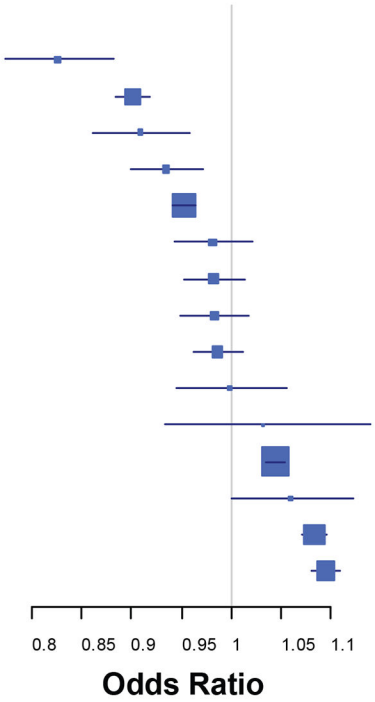

Figure 1. Decreased Crohn's disease risk for subjects carrying R130Q.

A PheWAS analysis was performed on the 23andMe database and evaluated the effect of the R130Q IL-13 variant across a select panel of immunological diseases. Associations between the R130Q IL-13 variant and the immunological diseases are represented as the odds ratios per increase in IL-13 (R130Q) allele number (center of solid square), the number of cases (area of the square) and 95% confidence intervals (extended lines) on a forest plot. The association test p-value reported was computed using a likelihood ratio test.

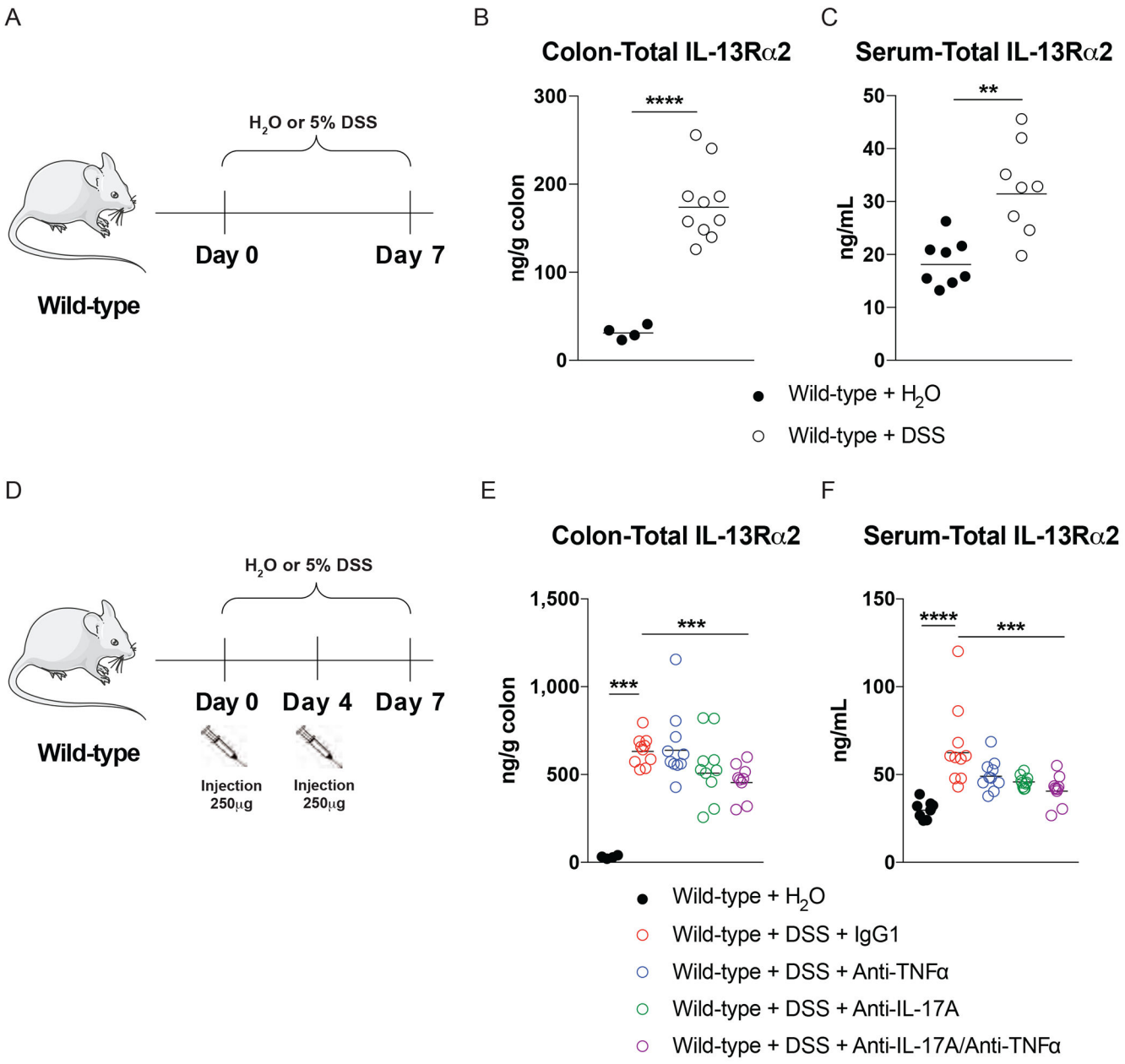

Figure 2. Increased production of IL-13Rα2 protein following DSS administration is partially dependent on TNFα and IL-17A *in vivo*.

(A) Wild-type mice were administered 5% DSS drinking water or normal drinking water for seven days. On day 7, mice were euthanized and IL-13Rα2 protein levels were measured in the (B) colon homogenates and (C) serum by ELISA. (D) Wild-type mice were given 5% DSS drinking water or normal drinking water for seven days. During the induction period of DSS-colitis, groups of mice were administered two intraperitoneal injections (250μg/mouse) of IgG1 isotype control (MOPC-21), anti-TNFα (XT22.11), anti-IL-17A (17F3), or anti-TNFα (XT22.11)/anti-IL-17A (17F3) antibodies. On day 7, mice were euthanized and IL-13Rα2 protein levels were measured in the (E) colon homogenates and (F) serum by ELISA. Experimental results are displayed showing the geometric mean. Statistical

significance was determined by Student's t-test (B and C) or One-way ANOVA (E and F) where **p<0.01, **p<0.001, and ****p<0.0001. Data are pooled from two independent experiments. (B and C n = 4-10 mice/group; E and F n = 10 mice/group).

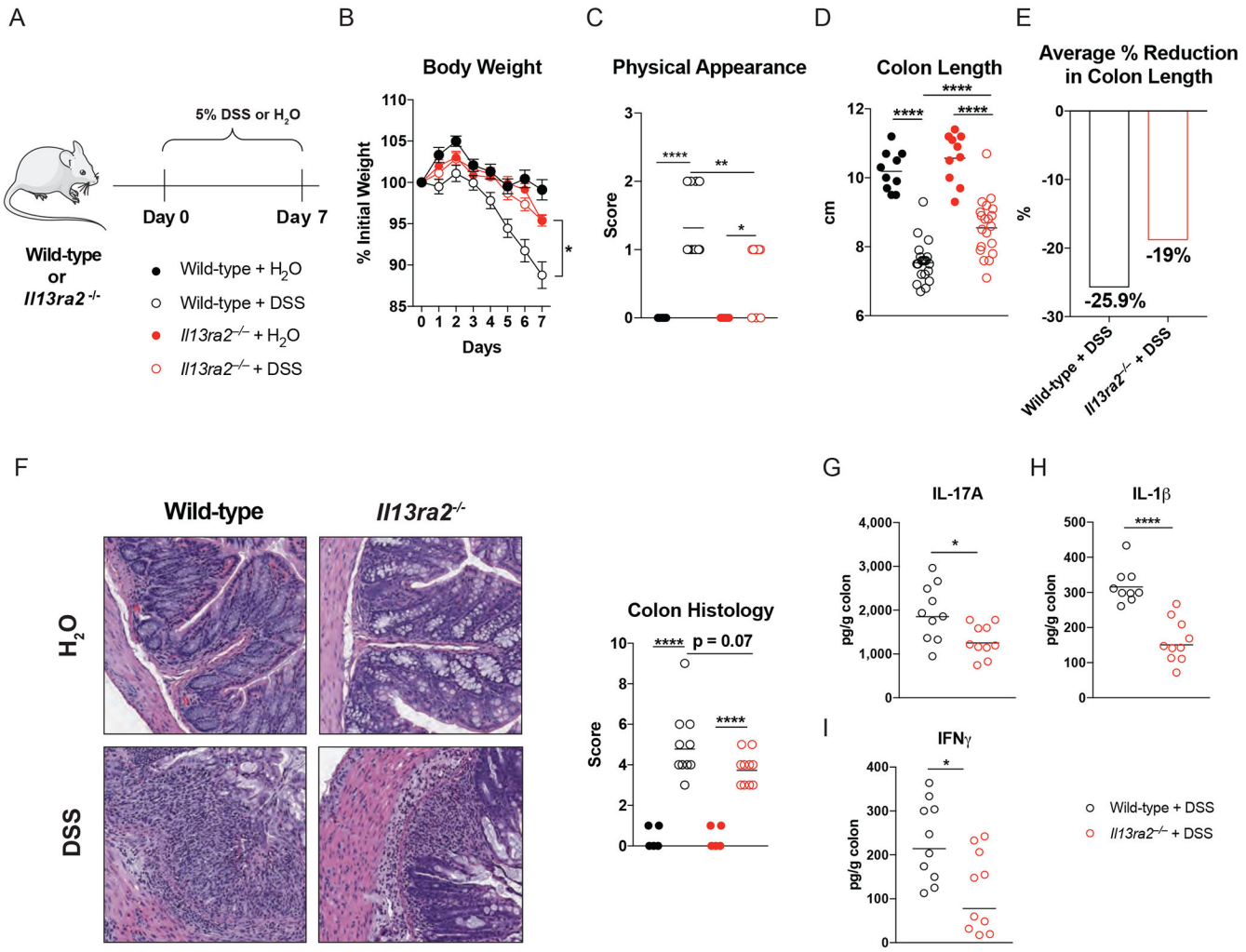

Figure 3. *Il13ra2*$^{-/-}$ mice are modestly protected from the induction of acute DSS-induced colitis.

(A) Wild-type and *Il13ra2*$^{-/-}$ mice were administered normal drinking water or 5% DSS drinking water for seven days. (B) The body weights of all mice were monitored daily. After seven days of DSS administration, (C) the physical appearance was scored prior to euthanizing mice and harvesting colons. (D) The colon lengths were measured and (E) the average percent reduction in colon lengths of DSS treated mice over normal drinking water controls were calculated. Distal colon was embedded in paraffin, sectioned, and (F) stained with H&E and the pathology was scored. Colon homogenates were generated and protein concentrations of (G) IL-17A, (H) IL-1β, and (I) IFNγ were measured by multiplex assay. Experimental results are displayed as the geometric mean expect (D) is represented as the mean +/− S.E.M. Statistical significance was determined by One-way ANOVA where *p<0.05, **p<0.01, and ****p<0.0001. Data are pooled from 2 independent experiments (B, C, D, E, F, G, H , and I n = 10-20 mice per group).

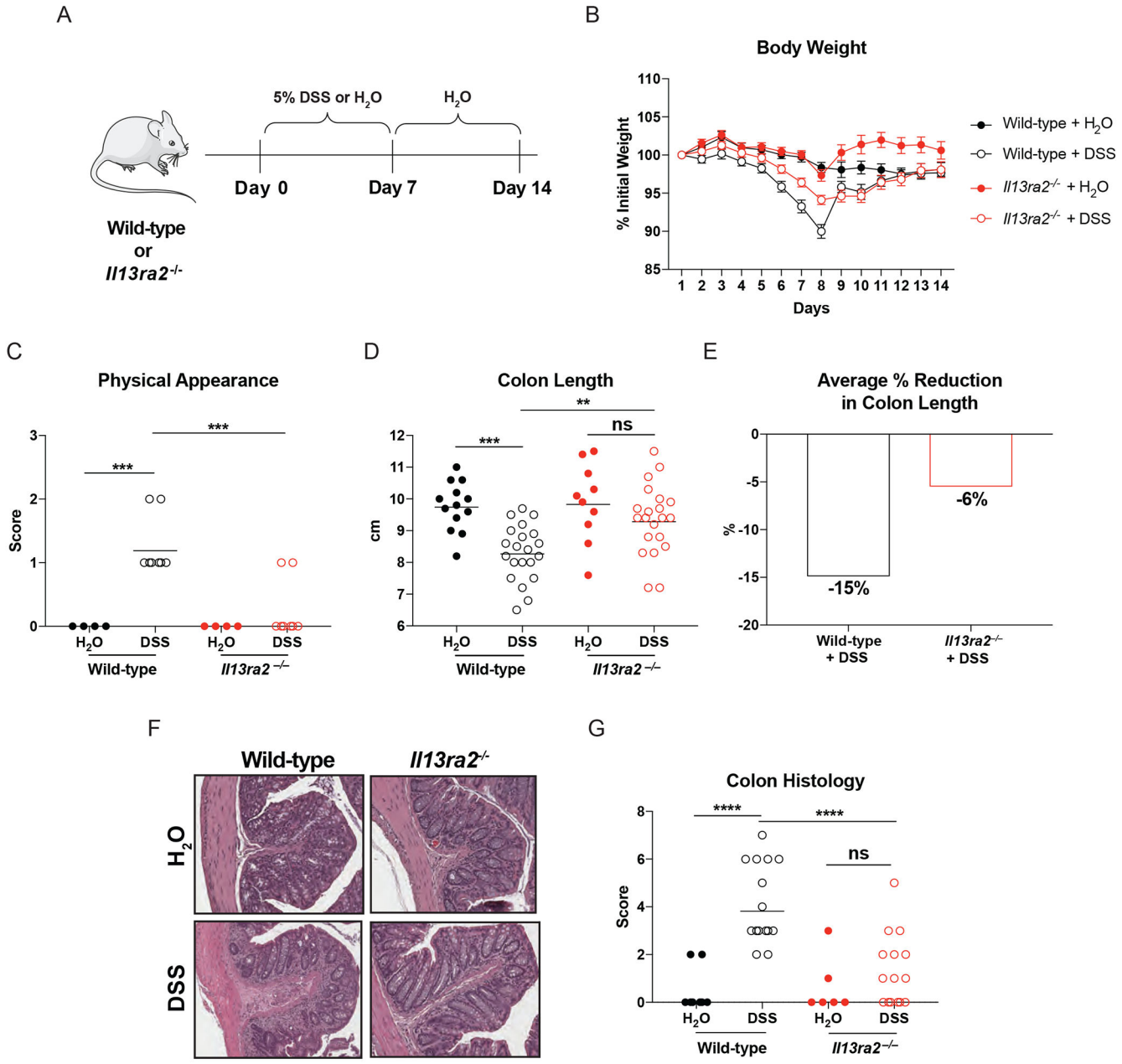

Figure 4. The absence of IL-13Rα2 promotes tissue injury recovery following DSS-induced colitis.

(A) Wild-type and *Il13ra2*$^{-/-}$ mice were given normal drinking water or 5% DSS drinking water for seven days. Then all mice were administered normal drinking water for seven days. (B)The body weights of mice were measured daily. On day 14, (C) the physical appearance of mice was scored. Then all mice were euthanized and (D) colon lengths were measured and (E) the average colon length reduction compared to untreated mice after seven days of recovery was calculated. Distal colons were paraffin embedded, sectioned, and stained with (F) H&E and (G) the pathology was scored. Experimental results are displayed showing the geometric mean except (B) is represented as the mean +/− S.E.M. Statistical

significance was determined by One-way ANOVA where *p<0.05, **p<0.01, and ****p<0.0001. Data are pooled from 3 independent experiments (B, D, E, F, and G n = 10-20 mice per group; C n = 5-10 mice per group).

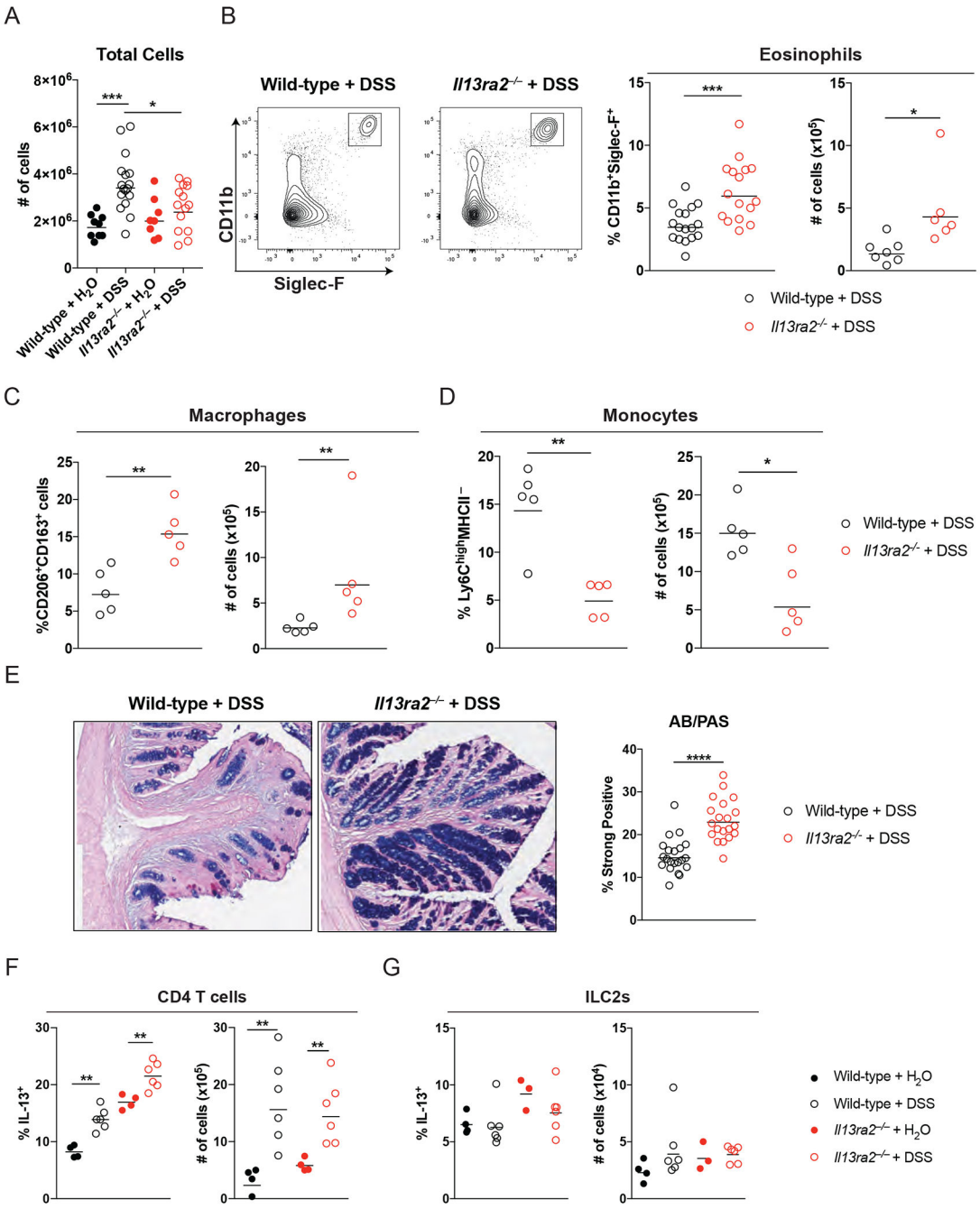

Figure 5. Increased type 2 immune cells and mucus production in the colon of *Il13ra2*$^{-/-}$ mice following recovery.

Wild-type and *Il13ra2*$^{-/-}$ mice were administered 5% DSS-drinking water or normal drinking water for seven days. Then all mice were placed on normal drinking water for a seven-day recovery period. On day 14, (A) leukocytes from the colonic lamina propria were isolated from wild-type and *Il13ra2*$^{-/-}$ mice, and the (B) frequency and number of CD11b^{+}Siglec-F^{+} eosinophils were determined by flow cytometry. (C) The frequency and total number of CD206^{+}CD163^{+} macrophages were determined by flow cytometry. (D) The frequency and total number of Ly6C^{+}MHCII^{-} monocytes were determined by flow

cytometry. (E) Colons from wild-type and *Il13ra2*$^{-/-}$ mice were stained with Alacian Blue Periodic Acid-Schiff and quantitated on day 14. On day 14, freshly isolated leukocytes from the colonic lamina propria were stimulated *ex vivo* with PMA (50ng/mL)/lonomycin (500ng/mL) for 3 hours at 37°C and (F) the frequency and total numbers of IL-13^{+} CD4^{+}TCRβ^{+} T cells and (G) ILC2s (gated on CD90.2^{+}CD4^{-} cells) were determined by flow cytometry. Experimental results are displayed showing the geometric mean. Statistical significance was determined by One-way ANOVA where *p<0.05, **p<0.01, ***p<0.001, and ****p<0.0001. Data are pooled from 2 independent experiments (A n = 9-17 mice per group; B n = 6-15 mice per group; C n = 5-6 mice per group; D n = 6 mice per group; E = 20 mice per group; F and G n = 3-6 mice per group).

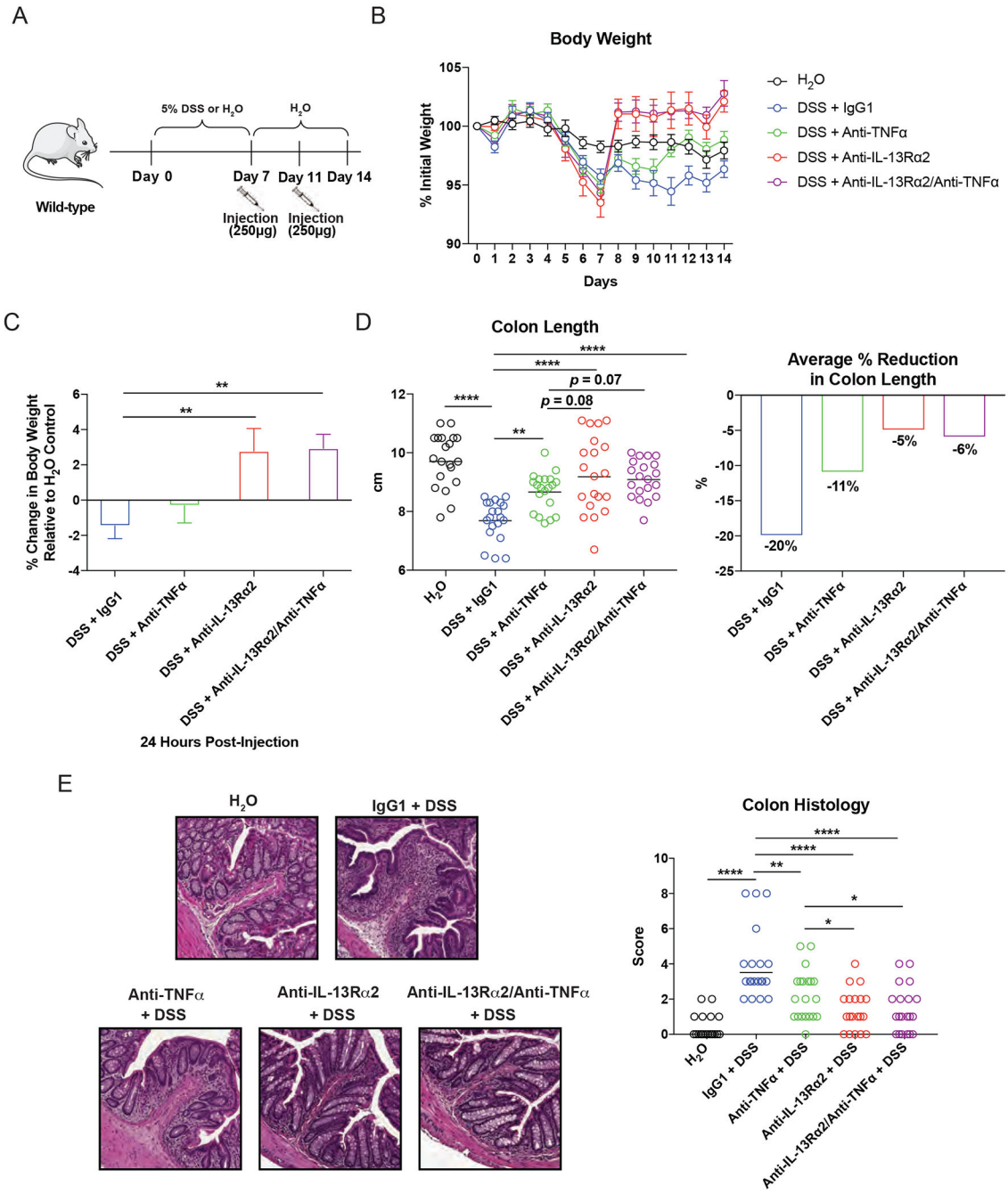

Figure 6. Therapeutic blockade of IL-13Rα2 promotes recovery from colitis.

Wild-type mice were administered 5% DSS-drinking water or normal drinking water for seven days. Then all mice were placed on normal drinking water for seven days. (A) On days seven and 11, mice were administered 250μg/mouse of anti-TNFα, anti-IL-13Rα2, or both anti-TNFα/anti-IL-13Rα2. Mice were assessed for disease severity by (B) monitoring body weight daily, (C) relative change in body weight compared to water controls 24 hours post-injection, (D) length of the colon and the average percent reduction in colon length. Distal colons were stained with (E) H&E and the pathology was scored. Experimental

results are represented as the geometric mean. Statistical significance was determined by One-way ANOVA where **p<0.01 and ****p<0.0001. Data are pooled from 2 independent experiments (n = 20 mice per group).

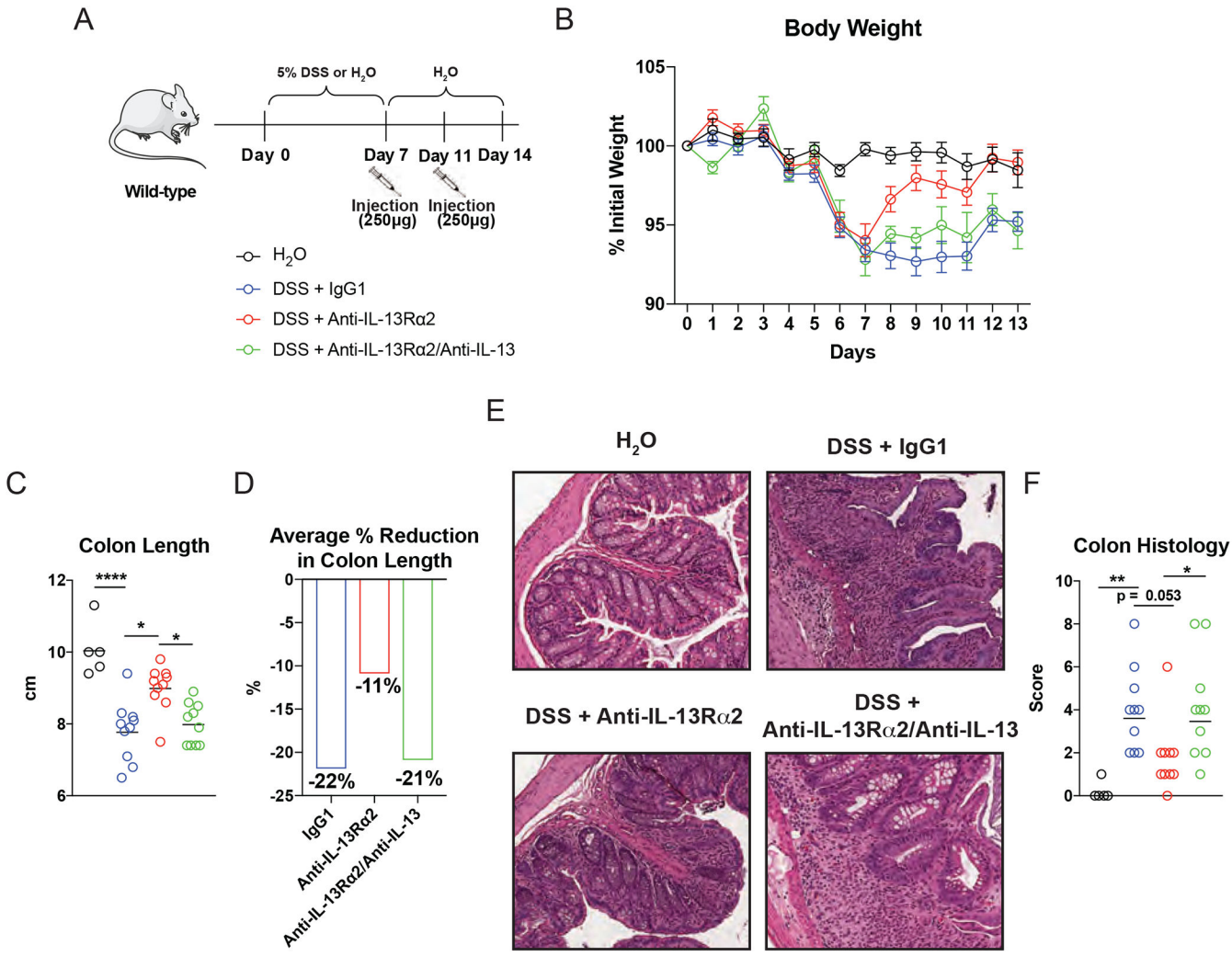

Figure 7. Recovery from acute DSS-induced colitis is mediated by IL-13.

Wild-type mice were administered 5% DSS drinking water or normal drinking water for days. Then all mice were placed on normal drinking water for a seven-day recovery period. (A) On days seven and 11, mice were administered 250µg/mouse of anti-IL-13Rα2, anti-IL-13Rα2/anti-IL-13, or IgG1 isotype control. (B) Body weights of mice were recorded daily throughout the induction and recovery periods. Mice were euthanized on day 14 and (C) colons were harvested and the lengths were measured. (D) The average percent reduction in colon length were calculated. Distal colons were stained with (E) H&E and the pathology was (F) scored. Experimental results are represented as mean +/− standard error. Statistical significance was determined by One-way ANOVA where *p<0.05, **p<0.01, and ****p<0.0001. Data are pooled from 2 independent experiments (n = 5-10 mice per group).